IOPscience iopscience.iop.org

Home Search Collections Journals About Contact us My IOPscience

Study of the correlation between radiative and non-radiative recombination channels in silicon

This article has been downloaded from IOPscience. Please scroll down to see the full text article.

2002 J. Phys.: Condens. Matter 14 13223

(http://iopscience.iop.org/0953-8984/14/48/372)

View the table of contents for this issue, or go to the journal homepage for more

Download details:
IP Address: 171.66.16.97
The article was downloaded on 18/05/2010 at 19:17

Please note that terms and conditions apply.

INSTITUTE OF PHYSICS PUBLISHING JOURNAL OF PHYSICS: CONDENSED MATTER

J. Phys.: Condens. Matter **14** (2002) 13223–13230 PII: S0953-8984(02)54010-8

Study of the correlation between radiative and non-radiative recombination channels in silicon

M Acciarri[1], C Cirelli[1], S Pizzini[1], S Binetti[1], A Castaldini[2] and A Cavallini[2]

[1] INFM and Department of Materials Science, University of Milano-Bicocca, Via Cozzi 53, Milano, Italy
[2] INFM and Department of Physics, University of Bologna, Viale Berti Pichat 6/2 Bologna, Italy

Received 27 September 2002
Published 22 November 2002
Online at stacks.iop.org/JPhysCM/14/13223

Abstract

The electronic properties of the recombination centres responsible for radiative and non-radiative recombination processes in silicon are studied by injection-level-dependent diffusion length measurements. Measurements were performed, using a spectral response method, on Czochralski silicon samples heat treated at 470 °C for different times in order to induce the thermal donor formation. The analysis of the injection level dependence of the carrier diffusion length using the Shockley–Read–Hall theory shows that the two fundamental recombination centres in these samples have an energy level located at 0.37 eV from the valence band and at 0.34 eV from the conduction band. The former centre is also responsible for the presence of the P line in the photoluminescence spectra. These results are in agreement with deep-level transient spectroscopy measurements carried out on the same samples.

(Some figures in this article are in colour only in the electronic version)

1. Introduction

There has recently been renewed interest in the possible development of silicon-based light-emitting devices compatible with standard silicon microelectronics technology. As silicon is an indirect gap semiconductor, dissolved impurities and defects, acting as radiative recombination centres, are the natural candidates for use to achieve this goal. While most metallic impurities are known to introduce deep levels at which non-radiative recombination occurs, extended defects are shown to give rise to radiative recombination effects [1].

Among other potential sources of room temperature light emission, compatible with standard silicon-based technology, we have studied silicon dioxide precipitates and old thermal donors, both of which could be generated in Czochralski (Cz) silicon by well defined heat treatments and present relatively intense emissions in a spectral range of technological interest. For both, however, a lack of knowledge still exists concerning the physics of radiative and

 © 2002 IOP Publishing Ltd Printed in the UK

non-radiative recombination processes, whose knowledge is preliminary to the development of light-emitting devices and this demands further investigation. In fact, the photoluminescence or electroluminescence yield in silicon is limited by non-radiative recombination paths and the development of silicon light-emitting devices calls for a better understanding of the physics of radiative and non-radiative recombination processes.

This can be achieve by considering at first that the total recombination lifetime τ_{tot} in silicon depends on three main recombination mechanisms [2]: the Shockley–Read–Hall (SRH) or multiphonon recombination, characterized by the lifetime τ_{SRH}, the radiative recombination characterized by τ_{rad} and the Auger recombination characterized by τ_{Auger}.

Thus,

$$\frac{1}{\tau_{tot}} = \frac{1}{\tau_{SRH}} + \frac{1}{\tau_{Auger}} + \frac{1}{\tau_{rad}} \tag{1}$$

which leads to the conclusion that the recombination process having the minimum lifetime is the predominant process.

In turn, the diffusion length (L_d) is related to the lifetime by the relationship

$$L_d = \sqrt{D\tau_{tot}}$$

where D is the diffusion coefficient of the current carriers.

Of these main recombination processes, the Auger one is dominant only in the case of high doping and very high injection. Therefore it can be neglected, at least in a first approach.

In many circumstances, the surface component of the SRH lifetime τ_s must be considered during lifetime or diffusion length measurements. Its importance depends, however, on the technique used and on the experimental conditions (e.g. surface passivation) and in some conditions it can be controlled or reduced.

Therefore, if the predominant non-radiative recombination process is the bulk SRH recombination, the analysis of the injection level dependence of τ_{SRH} can be used as a tool for defect recognition [3–6].

The SRH theory analyses a recombination process occurring at a discrete energy level at a depth E_t below the conduction band edge [7, 8], and allows one to obtain for the temperature- and injection-dependent carrier lifetime $\tau_{SRH}(T, h)$ the following well known equation (for an n-type semiconductor):

$$\tau_{SRH} = \frac{\tau_{n0}\left[h + \exp\left(\frac{2(E_i - E_F)}{kT}\right) + \exp\left(\frac{2E_i - E_t - E_F}{kT}\right)\right] + \tau_{p0}\left[1 + h + \exp\left(\frac{E_t - E_F}{kT}\right)\right]}{1 + h + \exp\left(\frac{2(E_i - E_F)}{kT}\right)} \tag{2}$$

where $h = \frac{\delta p}{n_0}$ is the injection level, $\frac{1}{\tau_{n0}} \equiv \sigma_n v_{th} N_t$ and $\frac{1}{\tau_{p0}} \equiv \sigma_p v_{th} N_t$ with σ_n, σ_p the electron and hole capture cross-sections, v_{th} the thermal velocity, N_t the impurity density, E_t the energy level of the impurity, E_i the intrinsic Fermi energy level, E_F the Fermi energy level, k the Boltzmann constant and T the temperature. In the presence of more than one recombination level, equation (2) must be written for each level and the total $1/\tau_{SRH,tot}$ is given by the sum of the $1/\tau_{SRH,n}$ for all the levels.

In turn, D also depends on the injection level and the temperature:

$$D = \frac{D_n D_p (2h + 1)}{D_p h + D_n (h + 1)} \tag{3}$$

where $D_{n,p} = \frac{kT}{e}\mu_{n,p}$ is the electron or hole diffusion constant, with $\mu_{n,p}$ the electron or hole mobility and e the electron charge [9].

Therefore, if the experimental injection level dependence of the lifetime or the diffusion length is analysed using the SRH recombination model, conclusions regarding the nature of the centres responsible for the non-radiative recombination might be obtained.

In this work, the case of thermal donors was chosen as an example of a system where the properties of the centres responsible for the radiative and non-radiative recombination processes and the evolution with the annealing time of their concentration are already known from photoluminescence (PL) and deep-level transient spectroscopy (DLTS) measurements [12]. The injection conditions were determined by comparing the calculated concentration of excess free carriers (δp) and the equilibrium majority carrier concentration (n_0). The carrier excess concentration was calculated following the procedure reported by Blood and Orton [9].

2. Experimental details

In the experiments, n-type ($\rho = 3.5$–$5\ \Omega$ cm) (100) Czochralski silicon samples (labelled Cz) with oxygen concentration of 18 ppma and carbon content below the FTIR detection limits (<0.1 ppma) were used as substrates. The samples were treated for times ranging from 8 to 64 h at 470 °C in order to induce thermal donor generation. Prior to any thermal treatment, the samples were CP4 and RCA etched and then were sealed under vacuum in quartz ampoules in order to avoid any possible metal contamination during the heat treatment. The oxygen content evolution with the annealing time was deduced from room temperature FTIR measurements. From the resistivity of all the samples, measured according the ASTM procedure F 723-88, the OTD concentration was then determined.

The diffusion length of the minority carriers was measured by a spectral response technique [10].

A chopped light beam, with variable wavelength, probes a collector junction (semitransparent Schottky junction). The short-circuit photocurrent is collected while varying the depth of the region where carrier generation occurs. Using optical excitation this is readily achieved by varying the wavelength of the incident light. The diffusion length is then obtained from the fitting of the experimental data as a function of penetration depth using the equation reported by Castaldini *et al* [10]. The penetration depth depends on the wavelength by the relation proposed by Nartowitz and Goodman [11]. More details of the technique are reported in [10].

The semitransparent Schottky barriers were realized by vacuum sputtering of a thin layer of Au. The ohmic contact on the back surface of the samples was created by brushing with an In–Ga paste.

The radiative recombination properties of the same samples were obtained from the analysis of the PL spectra, measured with a spectral resolution of 6 nm ($\Delta E = 4$ meV), using standard lock-in techniques in conjunction with a grating monochromator and InGaAs as a detector. For the excitation, a quantum well laser ($\lambda = 808$ nm) was used.

Finally, the parameters of the deep levels associated with majority carrier traps were obtained from the results of our previous work [12], where standard DLTS and minority carrier transient spectroscopy (MCTS) measurements were carried out by means of a SULA Tech. Inc. instrumentation. The temperature was varied from 12 to 350 K with reverse bias ranging from -4 to 0 V and a pulse width of from 1 to 10 ms.

3. Results and discussion

We report in table 1 the results of DLTS and MCTS experiments on as-grown and thermally annealed samples. It should be remarked that the shallow level at $E_c - 0.015$ eV was never observed before in DLTS measurements on thermally annealed samples and should correspond to the level of an exciton bound to a thermal donor [13, 14].

In these samples a pronounced degradation of the diffusion length (measured under low-injection conditions) was observed for annealing times lower than about 25 h (figure 1).

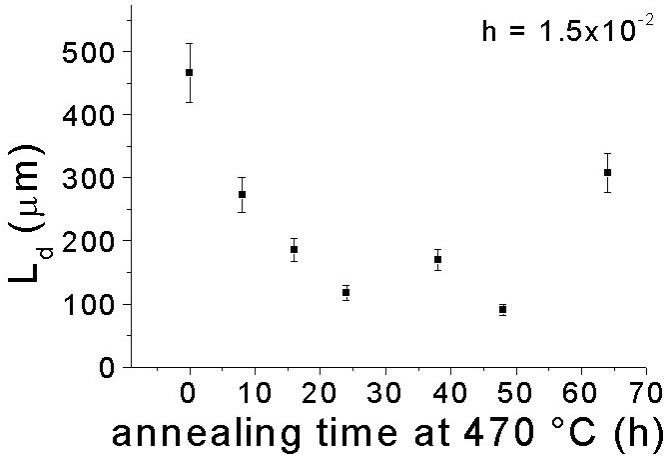

Figure 1. The evolution of the diffusion length of the minority carriers with the annealing time at 470 °C.

Table 1. Trap parameters obtained from the DLTS and MCTS experiments.

Samples	$E_c - E$ (eV)	σ_p (cm^2)	σ_n (cm^2)	N_T (cm^{-3})
As grown	0.16		1.6×10^{-18}	3.3×10^{12}
	0.23		6.3×10^{-18}	7.7×10^{11}
TT 470 °C	0.015		$(4.3–17) \times 10^{-21}$	
24 h	0.33		2.5×10^{-16}	9.2×10^{11}
TT 470 °C	0.34		6.2×10^{-17}	1.2×10^{12}
64 h				
	$E_v + E$ (eV)	σ_p (cm^2)	σ_n (cm^2)	N_T (cm^{-3})
TT 470 °C	0.37	1.75×10^{-18}		
24 h				

For longer times, a diffusion length recovery occurs. This behaviour seems not to have a direct correlation with the effect of the annealing time on the total concentration of TDs, as could be inferred from figure 2. In fact, the concentration of TDs increases almost linearly with time.

Figures 3 and 4 show the recombination lifetimes (calculated from the experimental values of L_d), as a function of the injection $h = \frac{\delta p}{n_0}$, for the as-grown sample and for the 24 h heat-treated sample, respectively. This last sample is considered representative of all the heat-treated samples before diffusion length recovery.

In both cases the fit (solid curves) was carried out via the standard SRH equation (equation (2)) using as fitting (free) parameters the electron and hole capture cross-sections σ and the trap density N. For the energy levels and the number of different traps, the results of DLTS experiments were used instead. For the as-grown sample the lifetime evolution was modelled using two energy levels at $E_c - 0.16$ eV and $E_c - 0.23$ eV, both of which, incidentally, disappear upon annealing at 450 °C. It could be remarked that a level at $E_c - 0.16$ eV could be systematically observed in as-grown commercial silicon wafers [15]. Considering that an in-depth profiling of this trap showed that it presents its maximum density close to the surface and that it disappears upon annealing, it was attributed to hydrogen–B complex induced by wet etching processes.

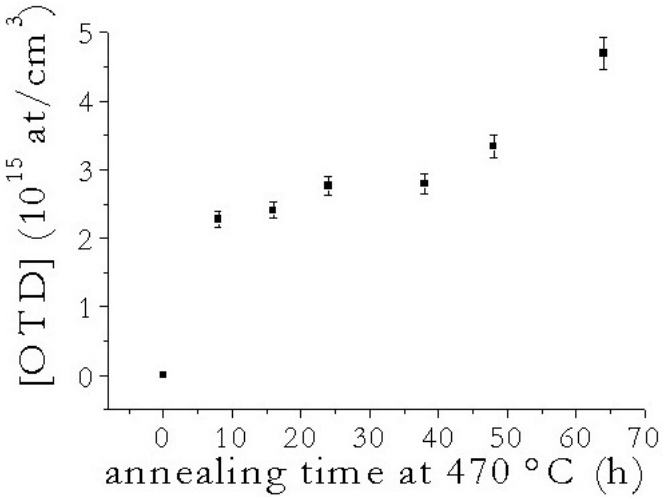

Figure 2. The evolution of the OTD concentration with the annealing time at 470 °C.

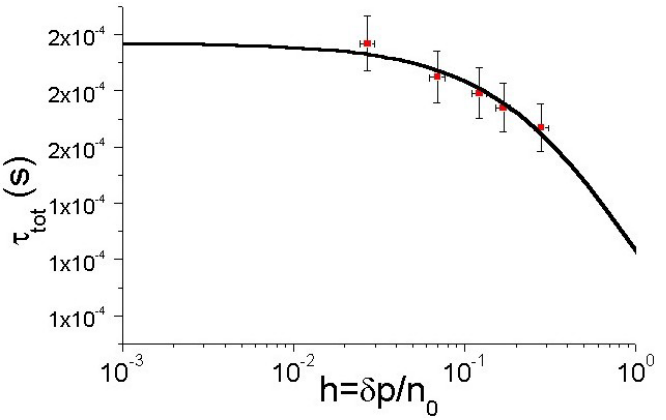

Figure 3. The evolution of the recombination lifetime with the injection level for the as-grown sample and the interpolation curve.

It was observed that a nice fitting was obtained and that the fitting parameters reported in table 2 are very close to the experimental values derived by DLTS and MCTS measurements.

The lifetime increase with increasing h, observed for all the heat-treated samples independently of their resistivity, can also be fitted by considering the presence of the two deep recombination centres observed in the DLTS measurements, located respectively at $E_c - 0.33$ eV and at $E_v + 0.37$ eV. In this case too the fitting parameters are in reasonable good agreement with the DLTS data; see table 2.

In order to evaluate the relative influence of these two traps on the recombination processes, and thus on the lifetime, we have compared in figure 5 the evolution with the annealing time of the lifetime and of the reciprocal of the intensity of the P line at 0.767 eV, which is always present in the PL spectra (see figure 6) in the presence of thermal donors [12].

The fact that the two curves show the same behaviour indicates that the trap responsible for the radiative recombination process is the same one as controls the lifetime evolution with the annealing time.

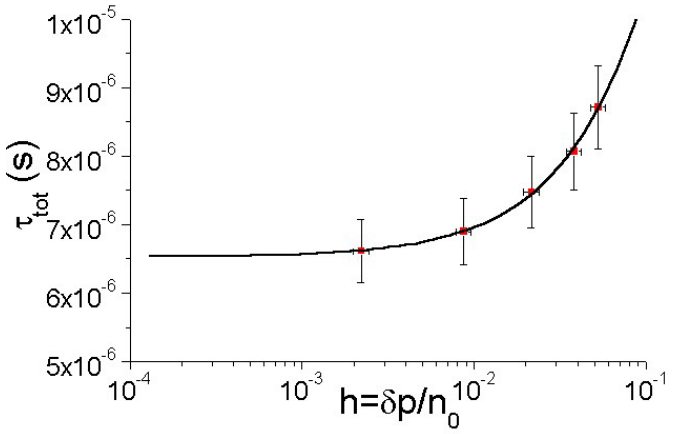

Figure 4. The evolution of the recombination lifetime with the injection level for the sample treated at 470 °C and the interpolation curve.

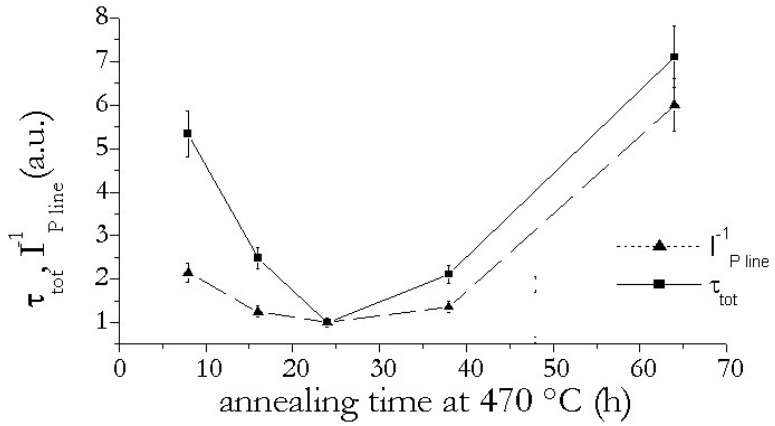

Figure 5. Normalized recombination lifetimes and the inverse of the P line intensity as a function of annealing time at 470 °C (the lines are only to guide the eyes).

Table 2. Trap parameters obtained from the interpolation of the recombination lifetime evolution with the injection level.

Samples	$E_c - E$ (eV)	σ_p (cm^2)	σ_n (cm^2)	N_T (cm^{-3})
As grown	0.16	6.4×10^{-16}	9.1×10^{-15}	3.3×10^{13}
	0.23	3.1×10^{-18}	5.6×10^{-18}	1.6×10^{12}
TT 470 °C 24 h	0.33	1.6×10^{-15}	2.1×10^{-16}	9.8×10^{11}
TT 470 °C 64 h	0.34	1.2×10^{-17}	3.4×10^{-17}	8×10^{12}
	$E_v + E$ (eV)	σ_p (cm^2)	σ_n (cm^2)	N_T (cm^{-3})
TT 470 °C 24 h	0.37	3.2×10^{-18}	6.8×10^{-18}	2.4×10^{15}

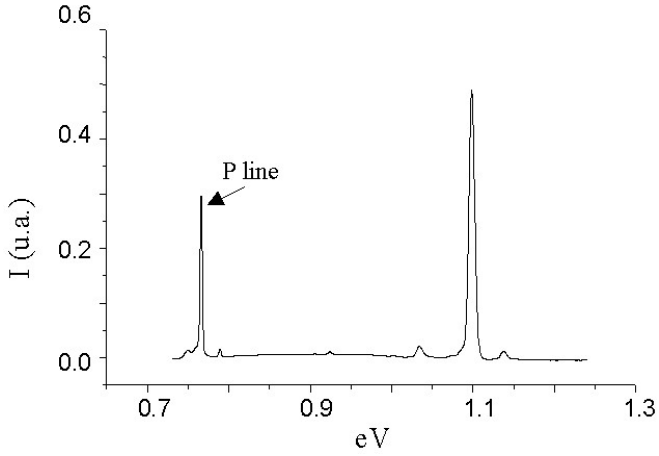

Figure 6. The PL spectrum of a sample after an annealing at 470 °C for 24 h ($T = 12$ K, $P = 6$ W cm^{-2}, $\Delta E = 4$ meV).

As a transition from a shallow trap at $E_c - 0.015$ eV to a deep trap at $E_v + 0.37$ eV was found to correspond almost exactly to the emission at 0.767 eV (P line) at 12 K, we had already suggested [12] that the trap at $E_v + 0.37$ eV is involved in the radiative recombination processes of samples containing thermal donors. Therefore, the lifetime of samples containing thermal donors is dominated by the deep trap at $E_v + 0.37$ eV.

Even more interesting are the results of DLTS and MCTS experiments reported in table 1, which are compared with the values of the capture cross-section and density of states obtained by fitting the experimental dependence of the lifetime. In this table only the fitting results obtained for the as-grown samples and those heat treated for 24 and 64 h are reported, as we only had DLTS or MCTS results for these. The capture cross-sections and the energy level values are indeed consistent for all the heat-treated samples.

It is quite remarkable that the fit data and the DLTS/MCTS results are significantly close, both for the case of the as-grown samples and for the heat-treated samples, with the presence in the annealed samples of three traps at $E_c - 0.015$ eV, $E_c - 0.33$ eV and at $E_v + 0.37$ eV, of which the second shows a significant increase in density above 24 h. The presence of this trap has, however, a minor effect on the diffusion length, as with these annealing times the recovery of the diffusion length does not reach the as-grown sample value.

From the annealing time dependence of the P trap density reported in figure 7, one could observe that the evolution of this trap follows quite nicely the evolution of the P line intensity.

4. Conclusions

In this work the electrical and optical properties of Cz silicon samples containing thermal donors have been studied. The analysis of the injection level dependence of the diffusion length was applied to the study of the recombination centres introduced during heat treatment. We found that the recombination centres mainly responsible for the diffusion length degradation have an energy level at $E_c - 0.34$ eV and one at $E_v + 0.37$ eV. This later centre is also responsible for the P line emission, as the evolution of its density with the annealing time follows the trend of the P line intensity. The energy position and the cross-section for both centres are in good agreement with the values obtained from DLTS/MCTS measurements.

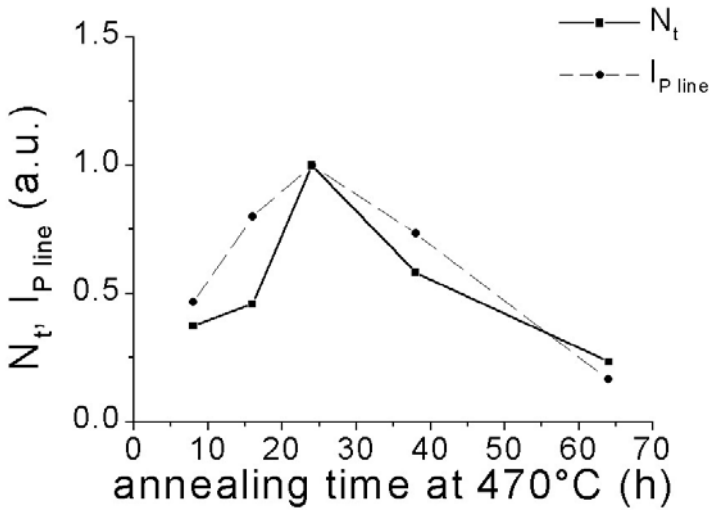

Figure 7. The normalized trap density with energy at $E_v + 0.37$ eV and the P line intensity as a function of annealing time at 470 °C (the lines are only to guide the eyes).

However, the injection-dependent lifetime analysis needs in any case a comparison with other techniques such as DLTS or PL spectroscopy, as during the fitting procedure some information about the centres responsible for the recombination is needed. In fact, as reported by Warta [16], the method is able to deliver conclusive results only if it is possible to investigate the defect in several differently doped samples. In our case only a limited resistivity range was investigated. A more complete study of defects can be carried out if the same analysis is carried out at different temperatures. At the moment an apparatus for execution of diffusion length measurements at different temperatures is under construction in our laboratory.

References

[1] Pizzini S, Guzzi M, Grilli E and Borionetti G 2000 *J. Phys.: Condens. Matter* **12** 10131
[2] Schroder D K 1998 *Semiconductor Material and Device Characterization* 2nd edn (New York: Wiley–Interscience) p 421
[3] Cavalcoli D, Cavallini A and Fraboni B 1994 *Phil. Mag.* B **70** 1095
[4] Kveder V, Kittler M and Schroter W 2001 *Phys. Rev.* B **63** 115208
[5] Schroder D K 2001 *Meas. Sci. Technol.* **12** R16
[6] Schmidt J and Cuevas A 1999 *J. Appl. Phys.* **86** 3175
[7] Shockley W and Read W T Jr 1952 *Phys. Rev.* **87** 835
[8] Hall R N 1952 *Phys. Rev.* **87** 387
[9] Blood P and Orton J W 1992 *The Electrical Characterization of Semiconductors: Majority Carriers and Electron States* (London: Academic)
[10] Castaldini A, Cavalcoli D and Cavallini A 2000 *Appl. Phys.* A **71** 305
[11] Nartowitz E S and Goodman A M 1985 *J. Electrochem. Soc.* **132** 2992
[12] Pizzini S, Binetti S, Leoni E, Le Donne A, Acciarri M and Castaldini A 2002 *Mater. Res. Soc. Symp. Proc.* **692** H6.30.1
[13] Newman R C 2000 *J. Phys.: Condens. Matter* **12** R335
[14] Heijmink Liesert B J, Gregorkiewicz T and Ammerlaan C A J 1992 *Phys. Rev.* B **46** 2034
[15] Castaldini A, Cavalcoli D, Cavallini A and Susi E 2002 *Appl. Phys.* A **75** 601
[16] Warta W 2002 *Sol. Energy Mater. Sol. Cells* **72** 389